AIAA 98-2693

# A Novel Flowfield Solution in a Rectangular Cavity Subject to Small Amplitude Oscillations

J. Majdalani
Marquette University
Milwaukee, WI 53233

**2nd AIAA Theoretical Fluid Mechanics Meeting**
June 15–18, 1998 / Albuquerque, NM

# A Novel Flowfield Solution in a Rectangular Cavity Subject to Small Amplitude Oscillations

J. Majdalani*
*Marquette University, Milwaukee, WI 53233*

**In a long, low aspect ratio, rectangular cavity, where transmission of a classic mean flow is permitted through compliant walls, a wave-induced time-dependent field is established when low amplitude, sinusoidal pressure oscillations with nonzero mean are introduced. An accurate solution is extracted for the time-dependent field by way of small parameter perturbations. Contingent upon small pressure wave amplitudes, Navier-Stokes equations are normalized and linearized to the order of the blowing Mach number, a typically small quantity, to yield the interaction equations governing the time-dependent velocity field. The latter is decomposed into irrotational and solenoidal fields that are coupled through Dirichlet-type boundary conditions. Solving for the rotational field from the momentum equation employs separation of variables and multiple scale expansions based on the reciprocal of the kinetic Reynolds number. A uniformly valid solution is formulated for the time-dependent field, disclosing thereon the character of the acoustic boundary layer developed from traveling waves that decay when distanced from the wall. The rate of decay is found to depend on a viscous similarity parameter, revealing that deeper penetration of rotational waves is possible at low viscosity. Characterization of the rotational boundary layer region is included in addition to a standard error analysis to ascertain the order of the truncation error associated with the analytical derivation. In the absence of an exact solution to rely on, results are verified through comparisons to highly accurate numerical predictions.**

## I. Introduction

WHEN harmonic disturbances are introduced inside a rectangular cavity with compliant walls, a rotational component of the time-dependent velocity is produced along with the plain, irrotational, acoustic field. The resulting time-dependent field is quite challenging to analyze since it must include the influence of the steady flow component. The traditional way to resolve the resulting coupled equations is paved with numerous mathematical obstructions that prevent exacting analytical solutions in finite form. Based on a technique implemented recently by the author,[1] an assault on the problem will be undertaken here. The method relies heavily on regular and multiple scale perturbation tools, making use of naturally occurring similarity parameters that happen to be small quantities. For example, in linearizing the Navier-Stokes equations, the ratio of the acoustic-to-mean pressure amplitude will be used as a primary perturbation parameter. The blowing Mach number at the wall will be found to be another instrumental perturbation parameter that is frequently encountered. Later, in resolving the rotational field, a small parameter reminiscent of the Stokes number will appear, providing a gauge to expand the rotational velocity in a series of progressively diminishing terms.

For the purpose of attaining a reliable solution, the current article starts in Sec. II with a brief description of the two-dimensional geometry and bulk fluid motion, along with a statement of the fundamental criteria whose violation is inadmissible. This is followed in Sec. III by a formulation of the linearized Navier-Stokes equations which rests on decomposing variables into mean and small time-dependent fluctuations. In the process, interaction equations that incorporate the influence of the mean flow are derived for the time-dependent flow to the order of the blowing Mach number. In Sec. IV, the classical mean flow velocity established inside a rectangular cavity is analyzed and shown to satisfy the principal requirements. The time-dependent field is decomposed in Sec. V into an acoustic, irrotational, pressure-driven, and a rotational, solenoidal, vorticity-driven elements. Equations governing each set are produced along with pertinent

*Assistant Professor, Department of Mechanical and Industrial Engineering. Member AIAA. 

boundary conditions. Unlike the acoustic set which can be readily resolved, the solenoidal solution demands a special treatment and is deferred to a separate section. Hence in Sec. VI, separation of variables and a careful scaling analysis precede the development of a uniformly valid solution to the rotational field. Attempts to elucidate particular features of the new finding and to explain its impact on the overall time-dependent solution are undertaken in Sec. VII where the time-dependent boundary layer is characterized. The global error associated with the analytical formulation is analyzed and the order of the truncation error is evaluated. Throughout this study, verifications are made at various stages by comparing analytical predictions to highly reliable computational data. Finally, several conclusions are reiterated in Sec. VIII by way of closing.

## II. Formulation of the Problem

### A. Geometry

The two-dimensional acoustic field is investigated in the half-space of a long rectangular cavity of length $L$, width $W$, and height $H$ ($W >> H$, $L >> H$), with one acoustically compliant membrane through which mean transmission of a compressible fluid (of kinematic viscosity $\nu_0$) occurs at a steady blowing speed of $V_b$. Compressible fluid entering the chamber at $y^* = H$ is induced to change course, swerve, and head downstream. As represented schematically in Fig. 1, the chamber is acoustically hard at the head end. The acoustic flowfield under investigation is choked at the downstream end due to a constriction in flow area (not shown). In addition, the lateral walls normal to the $x$ axis are impenetrable. Since the chamber width is larger than its height, variations in the $x$ direction are ignored. Under idealized conditions, the flow is perfectly symmetrical about the central plane $y^* = 0$. Taking advantage of symmetry, the domain investigation is limited to the half-space extending from the compliant wall to the central plane.

Superimposed on the mean fluid motion, a two-dimensional time-harmonic acoustic field of small amplitude (frequency $\omega_0$ and pressure amplitude $A_p$) is admitted. This acoustic environment can be induced externally or triggered naturally from internally propagating pressure disturbances. In the foregoing analysis, details of the acoustic source will not be of concern.

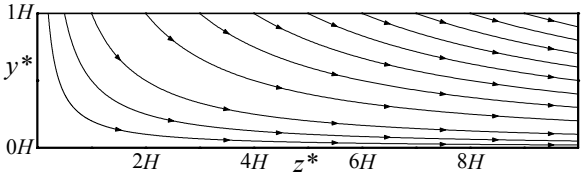


**Fig. 1 Chamber half-space showing mean flow streamlines.**

### B. Principal Criteria

In order to pursue a theoretical formulation of the time-dependent field, standard perturbation tools will be implemented in conjunction with a fundamental assumption of a low mean flow Mach number of $O(10^{-3})$. In common nonreacting flows characterized by a typical speed of sound of 350 m/s, the low Mach number criterion casts a limit of 2 m/s on the mean flow speed. In reality, this upper threshold for the Mach number is not too restrictive since, in many applications, it corresponds to a condition of intense mean flow transmission known as "hard blowing." Another basic assumption that must be tolerated to manage a solution constrains the acoustic pressure amplitude $A_p$ to remain small by comparison to the mean pressure $p_0$ at the chamber head end. The latter must be uniform in order to maintain rigor and consistency in comparing terms of various orders of magnitude arising in the perturbation process which rests strongly on the pressure wave amplitude, $A_p / p_0$, a gauge to which other quantities are compared. This criterion is found to be contingent upon a geometrical restriction of $L/H < 100$. When these criteria are met, the foregoing analysis will be applicable everywhere except near the choked end.

## III. Equations of Motion

### A. Conservation Laws

Invoking Stokes' hypothesis of zero bulk viscosity, assuming constant viscosity, and disallowing body forces, conservation of mass and momentum can be cast in dimensionless form into:

$$\frac{\partial \rho}{\partial t} + \nabla.(\rho \boldsymbol{u}) = 0 \tag{1}$$

$$\rho \frac{D\boldsymbol{u}}{Dt} = -\frac{\nabla p}{\gamma} + \frac{1}{Re}\left[\frac{4}{3}\nabla(\nabla.\boldsymbol{u}) - \nabla \times (\nabla \times \boldsymbol{u})\right] \tag{2}$$

where density and pressure are normalized by their mean values, $\rho_0$ and $p_0$, at the chamber head end, velocities are normalized by the speed of sound $a_0$, spatial coordinates are normalized by $H$, and time is made dimensionless by reference to the average time it takes for a pressure disturbance to travel from the compliant wall to the centerline, $(H/a_0)$. The Reynolds number $Re$ in Eq. (2) is $(a_0 H/\nu_0)$, $\gamma$ is the

ratio of specific heats, and $\boldsymbol{u}(y,z,t)$ is the total velocity, including both steady and unsteady components. Exacting the latter constitutes the main purpose of this article.

### B. Approach

The procedure consists of decomposing the internal flowfield into a steady and a time-dependent part. This is accomplished by writing each of the independent variables as a sum of their steady and time-dependent components. A small parameter perturbation scheme is suitable by virtue of the fundamental premise requiring the acoustic amplitude to be a small quantity relative to its mean counterpart.[2] In breaking the analysis into digestible pieces, we assume that the presence of time-dependent oscillations does not alter the general motion of the mean flow. This assumption can be later verified by realizing that terms that incorporate the time-dependent effects on the mean flowfield are indeed secondary. Experimentally, this assumption has been shown to be accurate in detailed analyses of the mean flow in analogous acoustic chambers.[3,4] Conversely, mean flow effects on the acoustic field are extraordinarily important and cannot be dismissed. Since superposition of the coupled elements is sought ultimately, equations that incorporate the coupling between steady and time-dependent components must be developed as well. Details are furnished below.

### C. Variable Decomposition

The local pressure can be expressed as the sum of its steady and acoustic components. Using, heretofore, asterisks to denote dimensional variables, and superscripts for perturbation orders, the dimensional pressure is split into

$$\begin{aligned} p^* &= p^{*(0)}(y^*,z^*) + p^{*(1)}(y^*,z^*,t^*) \\ &= p^{*(0)} + A_p f(y^*,z^*)\cos(\omega_0 t^*) \end{aligned} \tag{3}$$

where $p^{*(0)}$, subject to later verification, is taken to be a constant. In the time-dependent part of Eq. (3), $A_p$ defines the acoustic pressure amplitude, and $f$ is a normalized spatial function of $O(1)$. After normalizing by $p_0$, and substituting $p^{*(0)} \cong p_0$, Eq. (3) becomes

$$p = 1 + \varepsilon_w f(y,z)\cos(\omega_0 t^*) \tag{4}$$

where, $\varepsilon_w = A_p / p_0$, is the primary gauge parameter that provides a scale to which other terms can be compared. Density can be expanded in a similar way:

$$\rho(y,z,t) = \frac{\rho_0 + \rho^{*(1)}}{\rho_0} = 1 + \rho^{(1)}(y,z,t) \tag{5}$$

Velocity decomposition needs to be assessed carefully since its mean value is of the order of $V_b \boldsymbol{U}(y,z)$, where $\boldsymbol{U}(y,z)$ is a function of $O(1)$ to be described in Sec. IV. Expanding the dimensional velocity into

$$\boldsymbol{u}^*(y,z,t) = V_b \boldsymbol{U}(y,z) + \boldsymbol{u}^{*(1)}(y,z,t) \tag{6}$$

we normalize by the chamber speed of sound $a_0$ and find that the nondimensional counterpart is of the order of the wall Mach number; the latter is a secondary perturbation parameter by virtue of $\varepsilon_w < M_b << 1$. The normalized velocity becomes

$$\boldsymbol{u}(y,z,t) = M_b \boldsymbol{U}(y,z) + \boldsymbol{u}^{(1)}(y,z,t) \tag{7}$$

### D. Interaction Equations

Substituting Eqs. (4), (5) and (7) into Eqs. (1)-(2), one obtains, at the leading order expansion in the wave amplitude, a set for the steady flow motion:

$$\nabla . \boldsymbol{U} = 0 \tag{8}$$

$$\boldsymbol{U} . \nabla \boldsymbol{U} = \frac{1}{M_b Re}\left[\frac{4}{3}\nabla(\nabla . \boldsymbol{U}) - \nabla \times (\nabla \times \boldsymbol{U})\right] \tag{9}$$

Grouping terms that are comparable in magnitude to the first order in the wave amplitude, a linearized expansion of the interaction equations incorporating mean flow effects is attained (see Appendix A):

$$\partial \rho^{(1)} / \partial t + \nabla . \boldsymbol{u}^{(1)} = -M_b \nabla . (\rho^{(1)} \boldsymbol{U}) \tag{10}$$

$$\begin{aligned} \frac{\partial \boldsymbol{u}^{(1)}}{\partial t} &= M_b\left[\boldsymbol{u}^{(1)} \times (\nabla \times \boldsymbol{U}) + \boldsymbol{U} \times (\nabla \times \boldsymbol{u}^{(1)}) - \nabla(\boldsymbol{u}^{(1)} . \boldsymbol{U})\right] \\ &\quad - \frac{\nabla p^{(1)}}{\gamma} + \frac{1}{Re}\left[\frac{4}{3}\nabla(\nabla . \boldsymbol{u}^{(1)}) - \nabla \times (\nabla \times \boldsymbol{u}^{(1)})\right] \end{aligned} \tag{11}$$

Equations (10)-(11) reveal the intricate coupling between mean and time-dependent flow components which strongly affects the time-dependent solution character.

## IV. Mean Flowfield

### A. Velocity Field

The velocity field $\boldsymbol{U}$ can be determined from the stream function $\boldsymbol{S}_f = \Psi \boldsymbol{e}_x$ obtained for a flow inside a rectangular cavity[5] where $\boldsymbol{U} = \nabla \times \boldsymbol{S}_f$. For the classical stream function $\Psi(y,z) = -yz$, we get

$$\boldsymbol{U} = U_y \boldsymbol{e}_y + U_z \boldsymbol{e}_z = \frac{\partial \Psi}{\partial z}\boldsymbol{e}_y - \frac{\partial \Psi}{\partial y}\boldsymbol{e}_z$$
$$= -y\boldsymbol{e}_y + z\boldsymbol{e}_z \qquad (12)$$

which does satisfy Eqs. (8)-(9).

### B. Mean Pressure Correction

Having evaluated the velocity field from the stream function independently of mean pressure variations, one can use the steady momentum equation to deduce the pressure associated with the resulting field. Without incurring any loss in generality, one can set $p(y,z,t) = 1 + p_c(y,z) + p^{(1)}(y,z,t)$, where $p_c(y,z)$ is a spatial pressure correction term that we propose to determine. An auxiliary condition that must be met specifies that pressure at the chamber head end must be identical to the mean stagnation pressure where $p^{(0)} = 1 + p_c(0,0) = 1$, or $p_c(0,0) = 0$. The pertinent spatial correction can be obtained directly from Eq. (2) by direct substitution:

$$M_b \boldsymbol{U}.\nabla\left(M_b \boldsymbol{U}\right) = -\frac{\nabla p_c}{\gamma}$$
$$+\frac{1}{Re}\left[\frac{4}{3}\nabla\left[\nabla.\left(M_b \boldsymbol{U}\right)\right] - \nabla\times\left[\nabla\times\left(M_b \boldsymbol{U}\right)\right]\right] \qquad (13)$$

or

$$\nabla p_c / (\gamma M_b^2) = -\boldsymbol{U}.\nabla \boldsymbol{U} \qquad (14)$$

Equation (14) can be expressed in scalar form as

$$\frac{-1}{\gamma M_b^2}\frac{\partial p_c(y,z)}{\partial y} = U_y \frac{\partial U_y}{\partial y} = \frac{1}{2}\frac{\partial\left(U_y^2\right)}{\partial y} \qquad (15)$$

$$\frac{-1}{\gamma M_b^2}\frac{\partial p_c(y,z)}{\partial z} = \frac{1}{2}\frac{\partial\left(U_z^2\right)}{\partial z} \qquad (16)$$

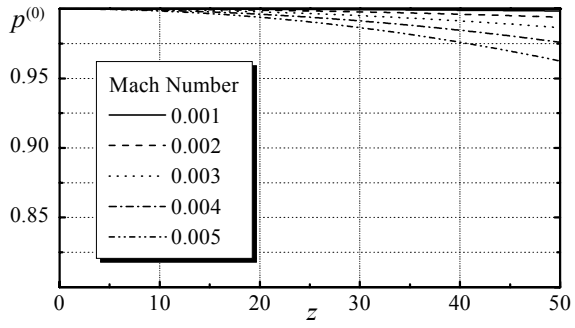


**Fig. 2 Steady pressure distribution for practical surface Mach numbers.**

and integrated to obtain, for $p_c(0,0) = 0$,

$$\frac{-1}{\gamma M_b^2} p_c(y,z) = \tfrac{1}{2} y^2 + \tfrac{1}{2} z^2 \qquad (17)$$

wherefrom

$$p^{(0)}(y,z) = 1 - \tfrac{\gamma}{2} M_b^2 \left(y^2 + z^2\right) \qquad (18)$$

Note that, in Eq. (18), the $y$-dependence can be safely ignored by comparison to the $z$-dependence, the former being smaller than unity, whereas $z^2$ varies from the order of unity to the order of $10^3$. Additionally, since $M_b$ is of $O(10^{-3})$, and $z$ is less than 100, the error in assuming a constant steady pressure is insignificant, being of order $M_b^2 z^2$. The corrected pressure distribution shown in Fig. 2, indicates that axial pressure variations are indeed negligible except in very long chambers with large Mach numbers. Since the Mach number in the majority of cases does not exceed 0.005, the assumption of a uniform mean value needed to represent the steady pressure distribution is well justified. Having, heretofore, established the steady flowfield character, its impact on the acoustic component is examined next.

## V. Time-Dependent Field

### A. Irrotational and Solenoidal Fields

The time-dependent velocity vector is decomposed into two vectors of distinct characters, one that is irrotational and one that is solenoidal[6]

$$\boldsymbol{u}^{(1)} = \boldsymbol{u}_{\text{irrotational}} + \boldsymbol{u}_{\text{solenoidal}} = \hat{\boldsymbol{u}} + \tilde{\boldsymbol{u}} \qquad (19)$$

contingent upon, $\nabla\times\hat{\boldsymbol{u}} = 0$, and $\nabla\cdot\tilde{\boldsymbol{u}} = 0$. Similar decomposition of a small amplitude disturbance into two modes of fluctuations, a pressure mode and a vorticity mode, has been accomplished previously by numerous authors, including Chu and Kovásznay,[7] Carrier and Carlson,[8], and Flandro.[9]

Plugging Eq. (19) back into Eqs. (10)-(11), the interaction equations for small disturbances can be written for each of the modes. The total time-dependent velocity field can be obtained, thereafter, by superimposing the solution vectors linearly. Designating the irrotational mode variables by the circumflex (^), and the solenoidal variables by the tilde (˜), we express the time-dependent quantities as

$$\boldsymbol{\omega}^{(1)} \equiv \nabla\times\boldsymbol{u}^{(1)} = \tilde{\boldsymbol{\omega}} \equiv \nabla\times\tilde{\boldsymbol{u}} \qquad (20)$$

$$p^{(1)} = \hat{p} \qquad (21)$$

$$\rho^{(1)} = \hat{\rho} \tag{22}$$

where vorticity is produced exclusively by the rotational mode and acoustic pressure is caused predominantly by the irrotational pressure mode. The pseudo-pressure generated by the vortical mode is ignored, being of second order in the wave amplitude.[7]

### B. Time-Dependent Equations of Motion

Substituting Eqs. (19)-(22) into the first order time-dependent set, given by Eqs. (10)-(11), yields the following two independent sets that are coupled through existing boundary conditions.

*1. Acoustic Model*

$$\partial\hat{\rho}/\partial t + \nabla.\hat{\boldsymbol{u}} = -M_b \nabla.\left(\hat{\rho}\boldsymbol{U}\right) \tag{23}$$

$$\frac{\partial\hat{\boldsymbol{u}}}{\partial t} = -\frac{\nabla\hat{p}}{\gamma} - M_b\nabla\left(\hat{\boldsymbol{u}}.\boldsymbol{U}\right) + \frac{4\nabla\left(\nabla.\hat{\boldsymbol{u}}\right)}{3Re} \tag{24}$$

*2. Vortical Model*

$$\nabla.\tilde{\boldsymbol{u}} = 0 \tag{25}$$

$$\frac{\partial\tilde{\boldsymbol{u}}}{\partial t} = M_b\left[\boldsymbol{U}\times\tilde{\boldsymbol{\omega}} - \nabla\left(\tilde{\boldsymbol{u}}.\boldsymbol{U}\right)\right] - \frac{\nabla\times\tilde{\boldsymbol{\omega}}}{Re} \tag{26}$$

### C. Auxiliary Conditions

In order to determine the total time-dependent velocity $\boldsymbol{u}^{(1)}$, irrotational and vortical components have to be determined separately by solving Eqs. (23)-(24), and Eqs. (25)-(26). Resulting solutions must be superimposed in a manner to correctly satisfy two existing boundary conditions: (1) Velocity adherence at the wall demanding the axial time-dependent component of the velocity to vanish at $y = 1$, thus yielding $\tilde{u}_z(1,z) = -\hat{u}_z(1,z)$, and (2) symmetry at $y = 0$, giving $\partial u^{(1)}(0,z)/\partial y = 0$.

### D. Irrotational Solution

Equations (23)-(24) can be cast into a set that possesses a classic solution presented in most textbooks treating acoustic waves. This can be accomplished by manipulating Eqs. (23)-(24), to eliminate one of the two dependent variables. The second order hyperbolic partial differential equation (PDE) that ensues, viz.

$$\frac{\partial^2\hat{p}}{\partial t^2} - \nabla^2\hat{p} = -M_b\left[\nabla.\left(\frac{\partial\hat{p}}{\partial t}\boldsymbol{U}\right) + \gamma\nabla^2\left(\hat{\boldsymbol{u}}.\boldsymbol{U}\right)\right] \tag{27}$$

can be solved to the first order in the Mach number by separation of variables. Since our original premise requires that $H/L << 1$, the lowest naturally excited frequencies will correspond to longitudinal oscillation modes, making it safe to neglect transverse modes of higher frequencies. For longitudinal waves in a rectangular chamber with constant cross-section, a multidimensional solution reduces to its one-dimensional form. The classical result for $\hat{p}(z,t)$ is expressed, hereunder, in complex variable notation

$$\hat{p}(z,t) = \varepsilon_w \cos\left(k_m z\right)\exp\left(-ik_m t\right) \tag{28}$$

where the wave number is given by $k_m = m\pi H/L$, $m = 1, 2, 3, \ldots$, and $m$ is the acoustic mode number. The acoustic velocity companion is determined directly from the momentum conservation Eq. (24) of order $M_b$. The result is

$$\hat{\boldsymbol{u}}(z,t) = i\frac{\varepsilon_w}{\gamma}\sin\left(k_m z\right)\exp\left(-ik_m t\right)\boldsymbol{e}_z \tag{29}$$

### E. Fundamental Vortical Equations

Using Euler's notation, we express rotational velocity and vorticity components in the following fashion:

$$\tilde{\boldsymbol{u}}(y,z,t) = \boldsymbol{V}(y,z)\exp\left(-ik_m t\right) \tag{30}$$

$$\tilde{\boldsymbol{\omega}}(y,z,t) = \boldsymbol{\varpi}(y,z)\exp\left(-ik_m t\right) \tag{31}$$

where

$$\boldsymbol{V}(y,z) = V_y\boldsymbol{e}_y + V_z\boldsymbol{e}_z \tag{32}$$

$$\boldsymbol{\varpi} = \nabla\times\boldsymbol{V} = \varpi\boldsymbol{e}_x \tag{33}$$

are complex functions. It follows that the vortical mass and momentum conservation equations, given by Eqs. (25)-(26), become

$$\nabla\cdot\boldsymbol{V} = 0 \tag{34}$$

$$i\boldsymbol{V} = \sigma\left[\nabla\left(\boldsymbol{V}.\boldsymbol{U}\right) - \boldsymbol{U}\times\boldsymbol{\varpi}\right] + \varepsilon\nabla\times\boldsymbol{\varpi} \tag{35}$$

where

$$\sigma = \frac{M_b}{k_m} = \frac{1}{Sr} = \frac{V_b}{\omega_0 H} < O\left(10^{-1}\right) \tag{36}$$

$$\varepsilon = \frac{1}{k_m Re} = \frac{1}{Re_k} = \left(\frac{\sqrt{\nu_0/\omega_0}}{H}\right)^2 < O\left(10^{-4}\right) \tag{37}$$

are naturally occurring dimensionless groupings representing the reciprocals of the Strouhal and kinetic Reynolds numbers, and satisfying

$$\varepsilon/\sigma = \nu_0/(V_b H) << 1 \tag{38}$$

Indubitably, $Re_k = 2\lambda_S^2$ is another form of the Stokes number, $\lambda_S$, which is expected to play a significant role in oscillatory flows. Equations (34)-(35) can be expanded in scalar form into

$$\frac{\partial V_y}{\partial y} + \frac{\partial V_z}{\partial z} = 0 \tag{39}$$

$$iV_y = \sigma\left[\frac{\partial}{\partial y}\left(V_y U_y\right) + U_z\frac{\partial V_y}{\partial z} + V_z\frac{\partial U_y}{\partial z}\right] - \varepsilon\left(\frac{\partial^2 V_y}{\partial z^2} - \frac{\partial^2 V_z}{\partial y \partial z}\right) \tag{40}$$

$$iV_z = \sigma\left[\frac{\partial}{\partial z}\left(V_z U_z\right) + U_y\frac{\partial V_z}{\partial y} + V_y\frac{\partial U_z}{\partial y}\right] - \varepsilon\left(\frac{\partial^2 V_z}{\partial y^2} - \frac{\partial^2 V_y}{\partial y \partial z}\right) \tag{41}$$

which reveal that direct analytical solutions to the coupled set are not tractable without exploitation of an important result that can be verified numerically, and proven theoretically, only *a posteriori*. Subject to later verification, the normal vortical velocity amplitude is assumed to be of $O(M_b)$ by comparison to the axial component. Being a smaller quantity, ignoring $V_y$ at the first perturbation expansion level of $V$ will not affect the solution which, let us recall, is only accurate to the first order in the Mach number. On that account, Eq. (41) becomes

$$iV_z = \sigma\left[\frac{\partial}{\partial z}\left(V_z U_z\right) + U_y\frac{\partial V_z}{\partial y}\right] - \varepsilon\frac{\partial^2 V_z}{\partial y^2} + O(M_b) \tag{42}$$

## VI. Vortical Solution

### A. Separation of Variables

Inserting Eq. (12) into Eq. (42), expanding and rearranging, one gets

$$z\frac{\partial V_z}{\partial z} = \left(\frac{i}{\sigma} - 1\right)V_z + y\frac{\partial V_z}{\partial y} + \frac{\varepsilon}{\sigma}\frac{\partial^2 V_z}{\partial y^2} \tag{43}$$

which suggests using separation of variables in order to investigate a solution of the type

$$V_z(y,z) = Y(y)Z(z) \tag{44}$$

When inserted back into Eq. (43), Eq. (44) allows splitting the original PDE into two linear ordinary differential equations (ODEs), coupled through a separation constant $\lambda_n$:

$$\frac{z}{Z}\frac{dZ}{dz} = \left(\frac{i}{\sigma} - 1\right) + \frac{y}{Y}\frac{dY}{dy} + \frac{\varepsilon}{\sigma}\frac{d^2 Y}{dy^2} = \lambda_n \tag{45}$$

where $\lambda_n$ must be strictly positive for a nontrivial outcome. For every $\lambda_n$, a solution $Z_n$ and $Y_n$ are manageable. Integration of the axially dependent equation is straightforward. The exact result is $Z_n(z) = c_n z^{\lambda_n}$, where $c_n$ is an integration constant associated with $\lambda_n$. Since the governing equation is linear, any linear combination of two or more solutions is also a solution, and one can write, in general, for all possible $\lambda_n$

$$V_z(y,z) = \sum_{\lambda_n} c_n z^{\lambda_n} Y_n(y) \tag{46}$$

where $\lambda_n$ must be determined from the no-slip boundary condition at the wall giving rise to the strong coupling between pressure and vorticity modes. As a consequence, rotational and irrotational components of the axial velocity cancel out at $y = 1$. This is achieved when, $\tilde{\boldsymbol{u}}_z = -\hat{\boldsymbol{u}}_z$, or

$$V_z(1,z) = -(\varepsilon_w/\gamma)i\sin(k_m z) \tag{47}$$

Inserting Eq. (47) into Eq. (46), writing out the MacLaurin series expansion for the Sine function, and equating summation terms results in

$$\sum_{\lambda_n} c_n z^{\lambda_n} Y_n(1) \equiv -\frac{\varepsilon_w}{\gamma} i\sum_{n=0}^{\infty}\frac{(-1)^n (k_m z)^{2n+1}}{(2n+1)!} \tag{48}$$

which holds true when $\lambda_n = 2n+1, n = 0,1,\ldots$, and

$$c_n = -\frac{\varepsilon_w}{\gamma} i\frac{(-1)^n (k_m)^{2n+1}}{(2n+1)!} \tag{49}$$

$$Y_n(1) = 1 \tag{50}$$

turning Eq. (46) into

$$V_z(y,z) = -\frac{\varepsilon_w}{\gamma} i\sum_{n=0}^{\infty}\frac{(-1)^n (k_m z)^{2n+1}}{(2n+1)!} Y_n(y) \tag{51}$$

In order to satisfy Eq. (45), the velocity eigenfunction $Y_n(y)$ remains to be determined from the two-point boundary value problem prescribed by

$$\varepsilon \frac{d^2 Y_n}{dy^2} + \sigma y \frac{dY_n}{dy} + \left[ i - (1+\lambda_n)\sigma \right] Y_n = 0 \qquad (52)$$

a second order ODE that is constrained by two naturally occurring auxiliary conditions:

$$Y_n(1) = 1 \text{ (no-slip)} \qquad (53)$$

$$\frac{dY_n(0)}{dy} = 0 \text{ (axial symmetry)} \qquad (54)$$

Equation (52) exhibits an exact closed form solution only at the undesirable cost of asymptotic linearization of the variable coefficient multiplying the first derivative. Attempts to extract a *uniformly valid* solution using perturbation techniques of the WKB and matched-asymptotic type turn out to be futile due to a logarithmic singularity at $y = 0$ that obstructs the matching process. Per contra, careful application of the derivative expansion method is successful in providing an accurate closed form solution that is valid in the entire solution domain. This approach is discussed below.

### B. Scaling Analysis

The first step for the derivative expansion method to work is the judicious identification of the scale at which order balance is achieved between locally significant terms in the governing ODE. To that end, we make the conjecture that, near the regular singularity

$$y = \varepsilon^{1/m} y_1^{-1/m} \qquad (55)$$

where $y_1$ is the relevant local scale and $m$ is a stretching exponent that must be carefully determined. The derivatives become

$$\frac{dY_n}{dy} = -m\varepsilon^{-1/m} y_1^{1+1/m} \frac{dY_n}{dy_1} \qquad (56)$$

$$\frac{d^2 Y_n}{dy^2} = m\varepsilon^{-2/m} y_1^{1+2/m} \left[ m y_1 \frac{d^2 Y_n}{dy_1^2} + (m+1)\frac{dY_n}{dy_1} \right] \qquad (57)$$

Substituting back into Eq. (52), we get

$$\varepsilon^{1-2/m} m^2 y_1^{2+2/m} \frac{d^2 Y_n}{dy_1^2} + m y_1 \left[ \varepsilon^{1-2/m} (m+1) y_1^{2/m} - \sigma \right] \frac{dY_n}{dy_1} + \left[ i - (1+\lambda_n)\sigma \right] Y_n = 0 \qquad (58)$$

which clearly indicates that $m = 2$ is a key stretching exponent that corresponds to a distinguished limit for which balance between various terms in Eq. (58) will exist. The rescaled equation becomes

$$4 y_1^3 \frac{d^2 Y_n}{dy_1^2} + 2 y_1 (3 y_1 - \sigma) \frac{dY_n}{dy_1} + \left[ i - (1+\lambda_n)\sigma \right] Y_n = 0 \qquad (59)$$

where the modified scale is

$$y_1 = \varepsilon y^{-2} \qquad (60)$$

Thus, when $y = O(\varepsilon^{1/2})$, representing the characteristic thickness of the inner layer near $y = 0$, the new variable $y_1$ will be of $O(1)$, which allows resolving accurately the rapid changes that can occur in such a small interval.

### C. Two-Variable Multiple-Scale Expansions

Having determined the form of the inner scale, a standard multiple-scale procedure can be implemented to transform Eq. (52) into a PDE that is function of two virtual variables, $y_0 = y$, and $y_1 = \varepsilon y^{-2}$. This requires expanding the derivatives in terms of the new variables

$$\frac{d}{dy} = \frac{\partial}{\partial y_0}\frac{dy_0}{dy} + \frac{\partial}{\partial y_1}\frac{dy_1}{dy} = \frac{\partial}{\partial y_0} - 2\varepsilon y_0^{-3}\frac{\partial}{\partial y_1} \qquad (61)$$

$$\frac{d^2}{dy^2} = \frac{\partial^2}{\partial y_0^2} + O(\varepsilon) \qquad (62)$$

Substituting back into Eq. (52), we obtain the following PDE:

$$\varepsilon \frac{\partial^2 Y_n}{\partial y_0^2} + \sigma y_0 \left( \frac{\partial Y_n}{\partial y_0} - 2\varepsilon y_0^{-3} \frac{\partial Y_n}{\partial y_1} \right) + \left[ i - \sigma(1+\lambda_n) \right] Y_n + O(\varepsilon^2) = 0 \qquad (63)$$

Next, $Y_n$ is expanded as a sum consisting of a leading order term and a series of consistently decreasing terms:

$$Y_n = Y_n^{(0)} + \varepsilon Y_n^{(1)} + O(\varepsilon^2) \qquad (64)$$

where $Y_n^{(0)}$ is the leading order term that we propose to find. Inserting the two-term expansion of $Y_n$ into Eq. (63), rearranging and collecting terms of $O(1)$ and $O(\varepsilon)$, we get, respectively

$$\varepsilon^0: \quad \sigma y_0 \frac{\partial Y_n^{(0)}}{\partial y_0} + \left[ i - (1+\lambda_n)\sigma \right] Y_n^{(0)} = 0 \tag{65}$$

$$\varepsilon: \quad \sigma y_0 \frac{\partial Y_n^{(1)}}{\partial y_0} + \left[ i - (1+\lambda_n)\sigma \right] Y_n^{(1)} = 2\sigma y_0^{-2} \frac{\partial Y_n^{(0)}}{\partial y_1} - \frac{\partial^2 Y_n^{(0)}}{\partial y_0^2} \tag{66}$$

Partial integration of Eq. (65) gives $Y_n^{(0)}$:

$$Y_n^{(0)}(y_0, y_1) = C_1(y_1) \exp\left\{ \left[ (1+\lambda_n) - i/\sigma \right] \ln y_0 \right\} \tag{67}$$

where the constant of integration $C_1$ can, in general, be a function of $y_1$; following traditional multiple-scale arguments, $C_1$ must be determined in a manner to ensure that $Y_n^{(0)}$ remains uniformly valid, viz., $Y_n^{(0)} > \varepsilon Y_n^{(1)}$, $\forall y$. This will occur when the first order term in Eq. (64) remains smaller that the leading order term in the series expansion for all $y$, and can only happen when the right hand side of Eq. (66) is zero. Differently stated, if the right hand side of Eq. (66) is not zero, the solution for $Y_n^{(1)}$ will include secular terms that make $Y_n^{(1)}$, in some regions of the solution domain, grow until $\varepsilon Y_n^{(1)}$ exceeds $Y_n^{(0)}$. Evidently, this condition cannot be tolerated since it violates the original premise and, furthermore, invalidates the regular perturbation expansion of $Y_n$ in a series of decreasing order terms. To suppress the source of secular terms, we set

$$2\sigma y_0^{-2} \frac{\partial Y_n^{(0)}}{\partial y_1} - \frac{\partial^2 Y_n^{(0)}}{\partial y_0^2} = 0 \tag{68}$$

where the derivatives are

$$\frac{\partial Y_n^{(0)}}{\partial y_1} = \frac{dC_1}{dy_1} \frac{Y_n^{(0)}}{C_1} \tag{69}$$

$$\frac{\partial^2 Y_n^{(0)}}{\partial y_0^2} = (\lambda_n - i/\sigma)\left[ (1+\lambda_n) - i/\sigma \right] \frac{Y_n^{(0)}}{y_0^2} \tag{70}$$

which, when substituted back into Eq. (68), yield

$$\frac{dC_1}{dy_1} - \frac{(\lambda_n - i/\sigma)\left[ (1+\lambda_n) - i/\sigma \right]}{2\sigma} C_1 = 0 \tag{71}$$

which can be easily solved for $C_1$:

$$C_1 = C_0 \exp\left\{ \frac{(\lambda_n - i/\sigma)\left[ (1+\lambda_n) - i/\sigma \right]}{2\sigma} y_1 \right\} \tag{72}$$

Recalling that $y_1 = \varepsilon y^{-2}$, the general, uniformly valid solution for $Y_n$ is

$$Y_n(y) = C_0 \exp\left\{ \left[ (1+\lambda_n) - i/\sigma \right] \ln y + \frac{\varepsilon(\lambda_n - i/\sigma)\left[ (1+\lambda_n) - i/\sigma \right]}{2\sigma y^2} \right\} + O(\varepsilon) \tag{73}$$

where $C_0$ can be determined readily from Eq. (53). Subsequently,

$$Y_n(y) = y^{(1+\lambda_n)} \exp\left\{ -\xi\left[ 1 - \sigma^2 \lambda_n (1+\lambda_n) \right](y^{-2} - 1)/2 - i\left[ \ln y + \xi\sigma^2 (1+2\lambda_n)(y^{-2} - 1)/2 \right]/\sigma \right\} + O(\varepsilon) \tag{74}$$

where $\xi = \varepsilon/\sigma^3$ is a nondimensional parameter that has a strong influence on the damping rate of $Y_n$.

### D. Analytical Solution in Infinite Series Form

Employing Eq. (74) in Eq. (51), letting $\eta = (y^{-2} - 1)/2$ for convenience, and summing up over all possible $\lambda_n$, renders

$$V_z(y,z) = -\frac{\varepsilon_w}{\gamma} i \sum_{n=0}^{\infty} \frac{(-1)^n (k_m z)^{2n+1}}{(2n+1)!} y^{(2n+2)} \times \exp\left\{ -\left[ 1 - \sigma^2 (2n+1)(2n+2) \right] \xi\eta - i\left[ \ln y + \xi\sigma^2 (4n+3)\eta \right]/\sigma \right\} + O(\varepsilon) \tag{75}$$

From Eq. (30), $\tilde{u}_z$ can be written in an infinite series form that clearly displays the leading order quantities and smaller quantities of $O(\sigma^2)$:

$$\tilde{u}_z(y,z,t) = -\frac{\varepsilon_w}{\gamma} i y \sum_{n=0}^{\infty} \frac{(-1)^n (k_m yz)^{2n+1}}{(2n+1)!} \times \exp\left\{ -\left[ 1 - \sigma^2 (2n+1)(2n+2) \right] \xi\eta - i\left[ \ln y + \xi\sigma^2 (4n+3)\eta \right]/\sigma - ik_m t \right\} + O(\varepsilon) \tag{76}$$

Fortunately, Eq.(76) is a rapidly converging series.

### E. Accurate Closed Form Equivalent

Equation (76) can be written in a closed form by disregarding small terms that do not affect the order of the error associated with the infinite series itself. The result is a practical, closed form equivalent

$$\tilde{u}_z(y,z,t) = -\frac{\varepsilon_w}{\gamma} iy \sin(k_m yz) \exp\left[-(1-2\sigma^2)\xi\eta - i(\ln y + 3\xi\sigma^2\eta)/\sigma - ik_m t\right] + O(\varepsilon) \quad (77)$$

### F. Graphical Verification

In order to verify that Eqs. (76) and (77) are concurrent, we first construct a solution for $\boldsymbol{u}^{(1)}$ by adding the irrotational component to $\tilde{u}_z$ in Eq. (19). This can be accomplished using either one of the two versions represented by Eqs. (76) and (77). In either case, the penetration depth $\delta$ of the resulting time-dependent velocity can be evaluated and compared to a reliable numerical solution to Eq. (42) achieved using a Runge-Kutta scheme of order seven.[10] In Fig. 3, a typical example is furnished that illustrates the excellent agreement between analytical predictions for $\tilde{u}_z$ and the numerical solution to Eq. (26). Since locating $\delta$ is sensitive to error accumulation, we overlay analytical predictions of $\delta$ versus $\sigma$ in Fig. 4 for a wide range of physical parameters as obtained from Eqs. (76) and (77). Reassuringly, no discernible discrepancies are detected anywhere, indicating that Eq. (77) can be exchanged for Eq. (76). This conclusion can be further confirmed by running a standard error calculation.

In addition to its simplicity and remarkable precision, Eq. (77) discloses the leading order terms which control the solution. These relate to the convection of unsteady vorticity by the mean flow in both axial and normal directions, time-dependent inertia, and viscous diffusion of time-dependent vorticity.

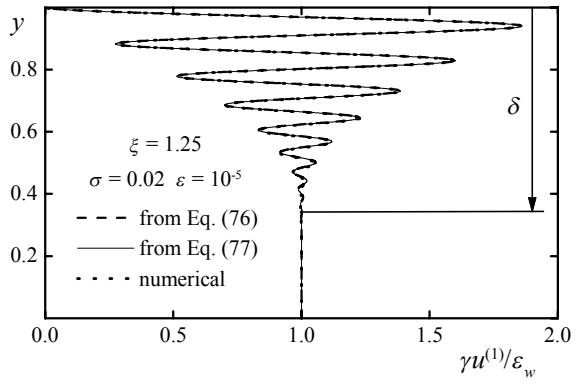


**Fig. 3 Virtually indistinguishable results for the total time-dependent velocity at chamber midspan as predicted from numerical, infinite series, and closed form expressions, corresponding to Eqs. (76) and (77).**

### G. Normal Velocity

The normal component $\tilde{u}_y$ can be determined in a manner to satisfy continuity. To that end, $\tilde{u}_z$ is used in Eq. (25) while an *ansatz* is proposed for $\tilde{u}_y$. From a conjectured form

$$\tilde{u}_y(y,z,t) = \frac{\varepsilon_w}{\gamma} G(y) \cos(k_m yz) \exp\left[-(1-2\sigma^2)\xi\eta - i(\ln y + 3\xi\sigma^2\eta)/\sigma - ik_m t\right] + O(\varepsilon) \quad (78)$$

the unknown function $G(y)$ must be determined to satisfy continuity. Substituting Eq. (77) and Eq. (78) into Eq. (25), the spatial function $G(y)$ is extracted in a manner to ensure that $\partial\tilde{u}_y/\partial y = -\partial\tilde{u}_z/\partial z$ is satisfied in the leading order terms. This occurs when

$$G(y) = -M_b y^3 \quad (79)$$

rendering

$$\tilde{u}_y(y,z,t) = -\frac{\varepsilon_w}{\gamma} M_b y^3 \cos(k_m yz) \exp\left[-(1-2\sigma^2)\xi\eta - i(\ln y + 3\xi\sigma^2\eta)/\sigma - ik_m t\right] + O(\varepsilon) \quad (80)$$

Clearly, the original assumption of $\tilde{u}_y/\tilde{u}_z = O(M_b)$ — leading to Eq. (42)— is justifiable. Furthermore, numerical computations of $\tilde{u}_y$ indicate that Eq. (80) is indeed accurate. Such comparisons with numerical predictions of $\tilde{u}_y$ are excluded here for brevity.

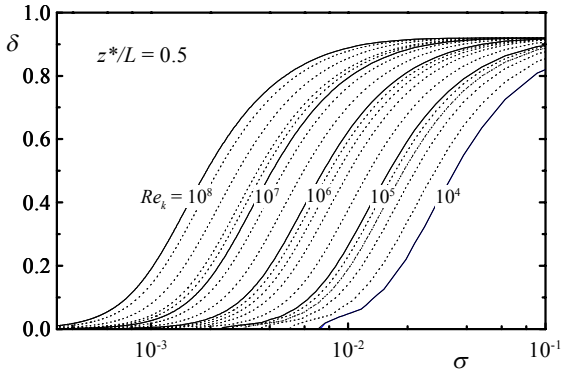


**Fig. 4 Penetration depth predictions from infinite series and closed form expressions, viz., Eqs. (76) and (77).**

## VII. Solution Character

### A. Total Time-Dependent Velocity

Superimposing rotational and irrotational velocity fields in Eq. (19), $u_z^{(1)}$ can be formulated at $O(M_b)$ :

$$u_z^{(1)}(y,z,t) = \frac{\varepsilon_w}{\gamma} i \exp(-ik_m t)\{\sin(k_m z) - y\sin(k_m yz) \times \exp[-(1-2\sigma^2)\xi\eta - i(\ln y + 3\xi\sigma^2\eta)/\sigma]\} \quad (81)$$

whose real part is

$$u_z^{(1)}(y,z,t) = \frac{\varepsilon_w}{\gamma}\left[\overbrace{\sin(k_m z)\sin(k_m t)}^{\text{irrotational part}} - \overbrace{\underbrace{y\sin(k_m yz)\exp(-\zeta)}_{\text{rotational amplitude}}\ \underbrace{\sin(k_m t + \Phi)}_{\text{wave propagation}}}^{\text{rotational part}}\right] \quad (82)$$

where

$$\zeta = \xi(1-2\sigma^2)(y^{-2}-1)/2 \quad (83)$$

$$\Phi = [\ln y + 3\xi\sigma^2(y^{-2}-1)/2]/\sigma \quad (84)$$

Evidently, $u^{(1)}$ is prescribed by $u_z^{(1)}$ which is a harmonic wave —traveling in the positive $y$ direction— characterized by a wave amplitude that diminishes exponentially with increasing distance from the wall. The vortical wave amplitude is actually controlled by two terms: an exponentially decaying term, made possible by inclusion of viscous dissipation, that decreases with the distance from the wall, and a sinusoidal term, made possible by inclusion of axial mean flow convection of unsteady vorticity, which varies harmonically with the distance from the head end, and also decreases with the distance from the wall. By inspection of the spatial damping function $\zeta$ in Eq. (77) and Eq. (82), increasing viscosity is found to cause the rotational wave to decay more rapidly, preventing a deeper inward penetration of vorticity. This effect is contrary to the boundary-layer "thickening" role played by viscosity in oscillatory flows between noncompliant parallel walls. Incorporation of blowing effects appears to alter the flow character quite dramatically. Results from Eq. (82) are congruent with numerical predictions which are achieved to a high order of accuracy (using a step size of $10^{-6}$ in conjunction with a nine-stage Runge-Kutta scheme that exhibits a global error of order seven).[10] This agreement shown in Fig. 5 causes graphical results to become visually indiscernible.

When, in Fig. 5, numerical and analytical velocity distributions are overlaid at eight evenly spaced times, only eight lines are perceived. Velocity time evolutions shown correspond to a full oscillation cycle and the first three pressure oscillation modes. The profiles are displayed at key axial positions corresponding to the location from the head end of the last harmonic pressure node.

A key feature captured very well by the analytical solution is that of the rotational velocity amplitude vanishing $m$ times at the $m^{\text{th}}$ pressure node. As shown in Figs. 5b-c, the rotational amplitude decays prematurely to zero somewhere between the wall and the central plane, corresponding to lines of zero unsteady vorticity. This peculiar effect, which can be attributed to the mean flow, downstream convection of

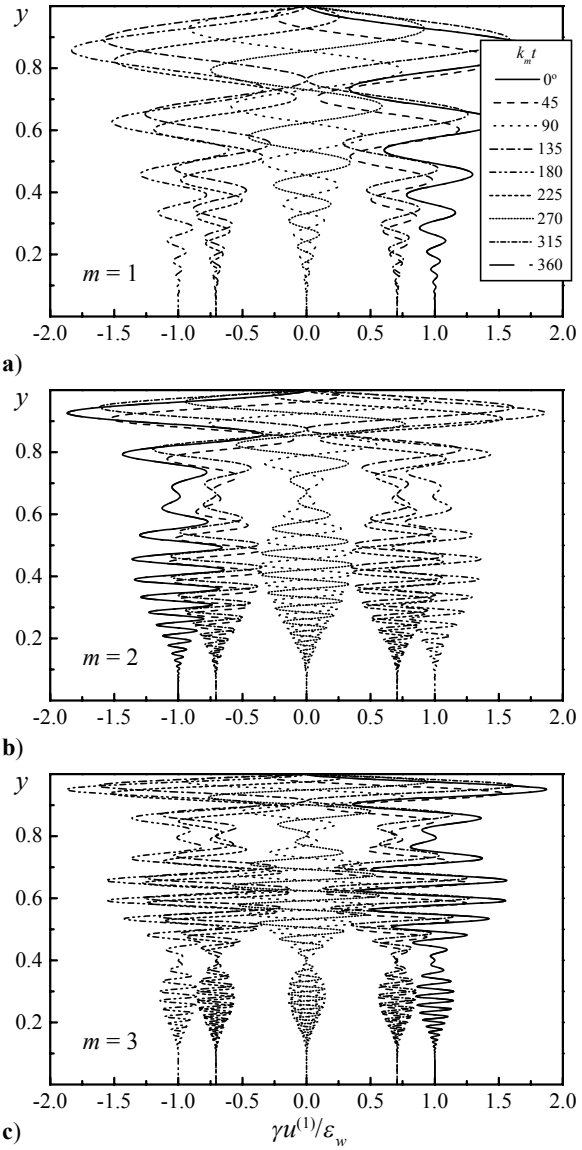


**Fig. 5 Evolution of time-dependent velocity shown for $Sr = 20m$ and $Re_k = 10^6 m$ at $z^*/L = (2m\text{-}1)/(2m)$.**

zero unsteady vorticity lines, is further evidence that the influence of the mean flow on the time-dependent field has been correctly incorporated.

### B. Acoustic Boundary Layer

We start by examining the rotational wave amplitude which controls the evolution of the time-dependent boundary-layer envelope:

$$\left\|\tilde{u}^{(1)}\right\| = \frac{\varepsilon_w}{\gamma} y \sin(k_m y z) \exp\left[-(1-2\sigma^2)\xi\eta\right] \qquad (85)$$

Defining the boundary layer to extend from the compliant wall to the point where 99% of the rotational wave component has vanished, the corresponding boundary layer thickness will be the distance from the wall to the point where $\left\|\tilde{u}^{(1)}\right\|$ becomes $\alpha \equiv 1\%$ of its irrotational counterpart. The normalized penetration depth $\delta$ extending from the wall to the edge of the boundary layer can, therefore, be calculated from $y_p = 1-\delta$, where

$$y_p \sin(k_m y_p z) \exp\left[-(1-2\sigma^2)\xi\eta\right] - \alpha\left|\sin(k_m z)\right| = 0 \quad (86)$$

Plots of $\delta$ versus $\sigma$ for a wide range of $Re_k$ are shown in Fig. 6 at two axial stations. The wide spread in the data makes it difficult to interpret the dependence of $\delta$ on actual physical parameters. This problem is alleviated by referring to Eq. (86) which clearly shows that the term involving exponential boundary layer decay is a strong function of a viscous damping parameter, $\xi$. This subtle realization motivates generating curves of $\delta$ versus $\xi$, for wide variations in $Re_k$. As shown in Fig. 7, entire families of curves, such as those shown in Fig. 4 and Fig. 6 at discrete axial stations, collapse splendidly into single curves per axial location. This significant result reveals that $\delta$ does not depend on $Re_k$ and $\sigma$ separately, but rather on $\xi = \omega_0^2 \nu_0 H V_b^{-3}$, a key similarity parameter that resembles, in importance, the Stokes number in oscillating flows over nontranspiring walls. However, unlike many similarity parameters, $\xi$ cannot be disclosed by standard dimensional analysis.

Figure 7 brings into focus the character of the oscillatory boundary layer over permeable walls. For instance, it is clear that $\delta$ depends on $\xi$, the pressure mode number and, to a lesser degree, on the axial station within the chamber. For large $\xi$, $\delta$ varies linearly with $\xi$, independently of $z$. Smaller $\xi$ imply larger penetration depths due to a smaller argument in the exponentially decaying term. In addition, increasing the blowing speed, or decreasing viscosity, frequency, or chamber height enhances the depth of penetration. Eventually, for sufficiently small $\xi$, $\delta$ tends asymptotically to a maximum fixed value per axial position.

In order to pinpoint this maximum possible penetration depth, $\delta_m$, occurring per axial station and mode number, we realize that, for the same geometry and blowing speed, larger penetration occurs in fluids with smaller viscosity. In the ideal case of zero viscosity, rotational waves face minimum friction and, thereby, travel the furthest distance from the wall. The asymptotic limit on the thickness of the boundary layer can thus be determined from the inviscid formulation of the penetration depth —which only depends on the axial station and pressure mode. Setting $\xi = 0$ in Eq. (86), we get

$$(1-\delta_m)\sin\left[k_m(1-\delta_m)z\right] - \alpha\left|\sin(k_m z)\right| = 0 \qquad (87)$$

The resulting expansion formula is

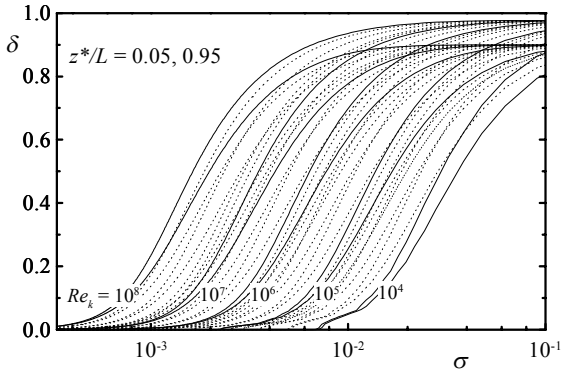


**Fig. 6 Locus of the rotational boundary-layer thickness at two axial stations.**

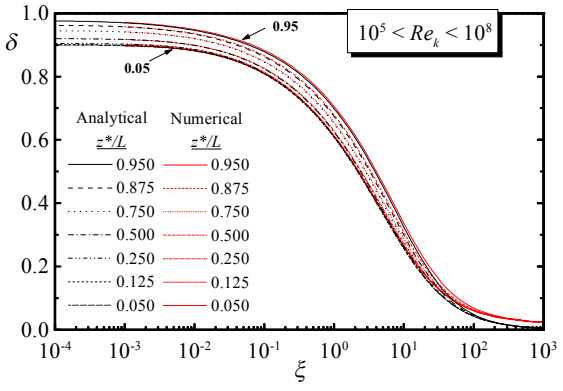


**Fig. 7 The boundary-layer thickness determined numerically and analytically at 7 discrete locations.**

$$\delta_m = 1 - \sqrt{\alpha \left| \sin(k_m z) \right| / (k_m z)} + O(1-\delta_m)^4 \qquad (88)$$

which allows predicting the inviscid depth of penetration quite accurately. A maximum truncation error of $O(10^{-4})$ corresponds to the largest value of $\delta_m$, which is 0.9 for $z = 0$. Having a smaller truncation error than $O(M_b)$, Eq. (88) can be exchanged for the numerical solution to Eq. (87). This is illustrated in Fig. 8 below for the first four acoustic modes where $\delta_m$ is shown to vary between 90 and 100% of the solution domain.

### C. Global Error Analysis

In order to ensure that no mistakes were committed in the derivation process, and to ascertain the order of the error associated with the final expression for the time-dependent velocity field, viz., Eq. (82), we calculate the maximum absolute error $E_m$ between the analytical prediction and the numerical outcome of Eq. (11) following Bosley's recommendation.[11] Since the absolute error defined here represents the deviation from the numerical solution, the latter is determined very accurately by using a seventh order Runge-Kutta scheme and a subinterval of $10^{-6}$. Assuming that the maximum absolute error exhibits the classical form

$$E_m = \left| u^{(1)}_{\text{numerical}} - u^{(1)}_{\text{analytical}} \right|_{\max} = K\varepsilon^{\kappa} \qquad (89)$$

then the order of the error, $\kappa$, can be determined from the slope of the linear least-squares fit to the data set generated by plotting $\log E_m$ versus $\log \varepsilon$ for different values of $\sigma$. As it can be inferred from Fig. 9, the order of the error approaches one asymptotically as $\varepsilon \to 0$, regardless of $\sigma$. Linear slopes obtained from least-squares lines with high correlation coefficients confirm that, indeed,

$$\kappa \xrightarrow[\varepsilon \to 0]{} 1 \qquad (90)$$

This reassuring observation leads us to conclude that the error associated with Eq. (82) is of $O(\varepsilon)$.

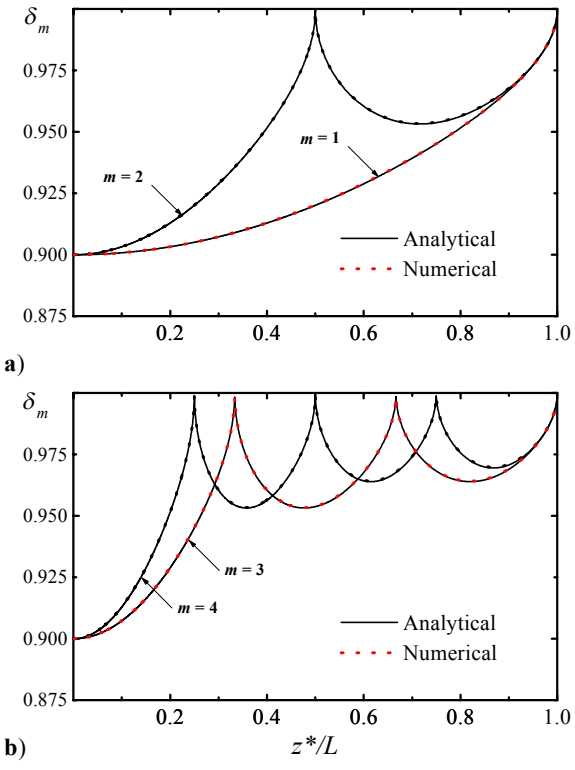


**Fig. 8 Trace of the maximum boundary-layer thickness for ideal fluids shown for the first four acoustic modes: (a) *m* = 1, 2 and (b) *m* = 3, 4.**

## VIII. Conclusions

In this article, the oscillatory field that results from harmonic pressure disturbances superimposed on the mean flow inside a rectangular cavity has been resolved. With regard to the time-dependent field, accurate expressions for the axial and normal velocity components have been extracted. The normal velocity is found to be small, namely, of the order of the blowing Mach number, by comparison to the axial counterpart. The latter dictates its character onto the total solution which represents a traveling wave that decays with distance from the wall. The rate of decay is found to be a strong function of a nondimensional parameter, $\xi = \omega_0^2 \nu_0 H V_b^{-3}$, that has a profound impact on the solution. At the outset, large viscosity leads to faster attenuation of the traveling wave envelope, and thereby, to smaller penetration depths of rotational waves. In addition to its strong dependence on $\xi$, the

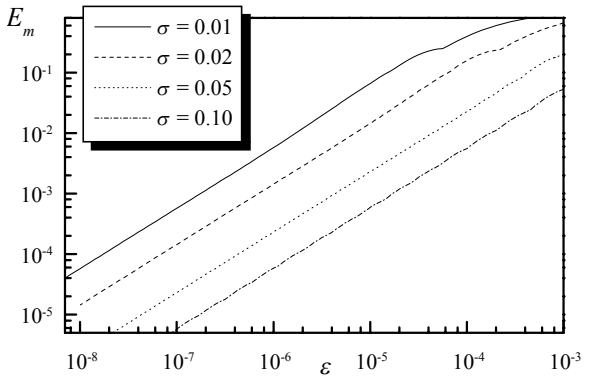


**Fig. 9 Maximum absolute error.**

penetration depth of rotational waves is found to depend on the acoustic mode number $m$, and on the distance from the head end, $z$. An accurate expansion formula is extracted for the maximum penetration depth associated with ideal fluids of small viscosity. Finally, a standard analysis of the maximum error associated with the analytical derivation validates the rigor of the perturbation approach and confirms the order of the reported truncation error.

## Appendix A: Linearization Details

Inserting the expanded variables into Eq. (1) yields

$$\partial\left(1+\rho^{(1)}\right)/\partial t+\nabla.\left[\left(1+\rho^{(1)}\right)\left(M_b\boldsymbol{U}+\boldsymbol{u}^{(1)}\right)\right]=0 \qquad \text{(A1)}$$

$$\nabla.\left(\underset{O(\tilde{\varepsilon}_w^0)}{M_b\,\boldsymbol{U}}+\underbrace{\boldsymbol{u}^{(1)}}_{O(\tilde{\varepsilon}_w^1)}+\underbrace{M_b\,\rho^{(1)}\boldsymbol{U}}_{O(\tilde{\varepsilon}_w^1)}+\underbrace{\rho^{(1)}\boldsymbol{u}^{(1)}}_{O(\tilde{\varepsilon}_w^2)}\right)+\partial\rho^{(1)}/\partial t=0 \qquad \text{(A2)}$$

Collecting terms to the first order in the wave amplitude, and ignoring smaller terms, one gets

$$\partial\rho^{(1)}/\partial t+\nabla.\left(\boldsymbol{u}^{(1)}+\rho^{(1)}M_b\boldsymbol{U}\right)=0 \qquad \text{(A3)}$$

which is Eq. (10). Inserting the expanded variables into Eq. (2), and recalling that $\nabla\cdot\boldsymbol{U}=0$, we get

$$\rho\partial\boldsymbol{u}/\partial t=\left(1+\rho^{(1)}\right)\partial\left(M_b\boldsymbol{U}+\boldsymbol{u}^{(1)}\right)/\partial t$$
$$=\partial\boldsymbol{u}^{(1)}/\partial t+\rho^{(1)}\partial\boldsymbol{u}^{(1)}/\partial t \qquad \text{(A4a)}$$

$$\boldsymbol{u}.\nabla\boldsymbol{u}=\left(M_b\boldsymbol{U}+\boldsymbol{u}^{(1)}\right).\nabla\left(M_b\boldsymbol{U}+\boldsymbol{u}^{(1)}\right)=M_b^2\boldsymbol{U}.\nabla\boldsymbol{U}$$
$$+M_b\boldsymbol{U}.\nabla\boldsymbol{u}^{(1)}+M_b\boldsymbol{u}^{(1)}.\nabla\boldsymbol{U}+\boldsymbol{u}^{(1)}.\nabla\boldsymbol{u}^{(1)} \qquad \text{(A4b)}$$

$$\rho\boldsymbol{u}.\nabla\boldsymbol{u}=\left(1+\rho^{(1)}\right)\boldsymbol{u}.\nabla\boldsymbol{u}=M_b^2\boldsymbol{U}.\nabla\boldsymbol{U}+M_b\boldsymbol{U}.\nabla\boldsymbol{u}^{(1)}$$
$$+M_b\rho^{(1)}\boldsymbol{u}^{(1)}.\nabla\boldsymbol{U}+M_b^2\rho^{(1)}\boldsymbol{U}.\nabla\boldsymbol{U}+\rho^{(1)}\boldsymbol{u}^{(1)}.\nabla\boldsymbol{u}^{(1)}$$
$$+M_b\boldsymbol{u}^{(1)}.\nabla\boldsymbol{U}+\boldsymbol{u}^{(1)}.\nabla\boldsymbol{u}^{(1)}+M_b\rho^{(1)}\boldsymbol{U}.\nabla\boldsymbol{u}^{(1)} \qquad \text{(A4c)}$$

$$-\nabla p/\gamma=-\nabla p^{(1)}/\gamma \qquad \text{(A4d)}$$

$$Re^{-1}\left[4\nabla\left(\nabla.\boldsymbol{u}\right)/3\right]=4Re^{-1}\nabla\left[\nabla.\left(M_b\boldsymbol{U}+\boldsymbol{u}^{(1)}\right)\right]/3$$
$$=4Re^{-1}\nabla\left(\nabla.\boldsymbol{u}^{(1)}\right)/3 \qquad \text{(A4e)}$$

$$-Re^{-1}\nabla\times\left(\nabla\times\boldsymbol{u}\right)=-Re^{-1}\nabla\times\left[\nabla\times\left(M_b\boldsymbol{U}+\boldsymbol{u}^{(1)}\right)\right]$$
$$=-Re^{-1}M_b\nabla\times\left(\nabla\times\boldsymbol{U}\right)-Re^{-1}\nabla\times\left(\nabla\times\boldsymbol{u}^{(1)}\right) \qquad \text{(A4f)}$$

Adding up Eqs. (A4a)-(A4f), we realize that the zero order terms yield back Eq. (9) associated with the steady field. Collecting terms to the first order in the wave amplitude, and disregarding smaller terms, we obtain

$$\partial\boldsymbol{u}^{(1)}/\partial t+M_b\boldsymbol{U}.\nabla\boldsymbol{u}^{(1)}+M_b\boldsymbol{u}^{(1)}.\nabla\boldsymbol{U}=-\nabla p^{(1)}/\gamma$$
$$+4Re^{-1}\nabla\left(\nabla.\boldsymbol{u}^{(1)}\right)/3-Re^{-1}\nabla\times\left(\nabla\times\boldsymbol{u}^{(1)}\right) \qquad \text{(A5)}$$

which by making use of the vector identity,

$$\left(\boldsymbol{U}.\nabla\right)\boldsymbol{u}^{(1)}+\left(\boldsymbol{u}^{(1)}.\nabla\right)\boldsymbol{U}=\nabla\left(\boldsymbol{u}^{(1)}.\boldsymbol{U}\right)$$
$$-\boldsymbol{u}^{(1)}\times\left(\nabla\times\boldsymbol{U}\right)-\boldsymbol{U}\times\left(\nabla\times\boldsymbol{u}^{(1)}\right) \qquad \text{(A6)}$$

leads to the leading order, time-dependent momentum equation, referred to in Sec. III as Eq. (11).

## References


[1]Majdalani, J., and Van Moorhem, W. K., "Improved Time-Dependent Flowfield Solution for Solid Rocket Motors," *AIAA Journal,* Vol. 36, No. 2, 1998, pp. 241-248.

[2]Van Dyke, M., *Perturbation Methods in Fluid Mechanics*, The Parabolic Press, Stanford, CA, 1975.

[3]Brown, R. S., Blackner, A. M., Willoughby, P. G., and Dunlap, R., "Coupling Between Acoustic Velocity Oscillations and Solid Propellant Combustion," *Journal of Propulsion and Power,* Vol. 2, No. 5, 1986, pp. 428-437.

[4]Shaeffer, C. W., and Brown, R. S., "Oscillatory Internal Flow Studies," Chemical Systems Div. Rept. 2060 FR, United Technologies, San Jose, CA, Aug. 1992.

[5]White, F. M., *Viscous Fluid Flow*, McGraw-Hill Book Company Inc., New York, 1991, pp. 135-136.

[6]Sommerfeld, A., *Mechanics of Deformable Bodies*, *Lectures on Theoretical Physics*, Section 20, Vol. II, Academic Press, New York, 1950, pp. 147-154.

[7]Chu, B. T., and Kovásznay, L. S. G., "Nonlinear Interactions in a Viscous Heat-Conducting Compressible Gas," *Journal of Fluid Mechanics,* Vol. 3, 1957, pp. 494-514.

[8]Carrier, B. T., and Carlson, F. D., "On the Propagation of Small Disturbances in a Moving Compressible Fluid," *Quarterly of Applied Mathematics,* Vol. 4, No. 1, 1946, pp. 1-12.

[9]Flandro, G. A., "Effects of Vorticity on Rocket Combustion Stability," *Journal of Propulsion and Power,* Vol. 11, No. 4, 1995, pp. 607-625.

[10]Butcher, J. C., *The Numerical Analysis of Ordinary Differential Equations*, *Runge-Kutta and General Linear Methods*, John Wiley & Sons, Great Britain, 1987, pp. 206-207.

[11]Bosley, D. L., "A Technique for the Numerical Verification of Asymptotic Expansions," *SIAM Review,* Vol. 38, No. 1, 1996, pp. 128-135.